The Na–Cu–O phase diagram in the Cu-rich part

Andrei B. Kulakov,[a,b,]* Andrei N. Maljuk,[a] Mikhail Sofin,[a] Chengtian T. Lin,[a] Bernhard Keimer,[a] and Martin Jansen[a]

[a] *Max-Planck-Institut für Festkörperforschung, Heisenbergstrasse 1, Postfach 800665, Stuttgart D-70569, Germany*
[b] *Institute of Solid State Physics, RAS, Chernogolovka, 142432 Moscow Distr., Russia*

Abstract

We report the thermogravimetry data of $NaCu_2O_2$ and $NaCuO$ compounds in Ar/O_2 gas mixtures with different oxygen contents accompanied by X-ray analysis. Preliminary synthetic approaches for compounds in the Na–Cu–O system were developed. Combined with X-ray diffractometry of a number of specimens synthesized with compositions corresponding to the oxygen-poor area of diagram, these data enabled us to determine the Cu-rich part of the Na–Cu–O phase diagram. The low-stability-limit line of $NaCu_2O_2$ in $\lg(pO_2)-1/T$ axes has been established. The Cu_2O–$NaCuO$ eutectic is considered as a possible flux for $NaCu_2O_2$ single crystal growth.
© 2004 Elsevier Inc. All rights reserved.

1. Introduction

The discovery of high temperature superconductivity in cuprates stimulated investigations of phase compatibilities in systems with the participation of copper oxides and cuprates. Nevertheless, the *M*–Cu–O phase diagrams (*M* = alkaline elements) have not been published till now, although numerous compounds are known in these systems. Perhaps, such investigations are lacking because of methodical difficulties to be met when dealing with high-reactivity compounds sensitive to moisture and (sometimes) oxygen, showing high volatility of the respective alkaline component and reactivity to all container materials at high temperatures.

A number of ternary compounds are known in the Na–Cu–O system, besides the two binary oxides of copper (CuO and Cu_2O [1]) and four stable oxides of sodium (Na_2O, Na_2O_2, NaO_2 [2] and NaO_3 [2,3]). The existence of the following compounds was established in this system: NaCuO [4], $NaCu_2O_2$ [5], $NaCuO_2$ [6–8] and $Na_6Cu_2O_6$ [9]. Several papers report on the

existence of Na_3CuO_2. Recently, Sofin et al. [10] reported on the synthesis of single-phase Na_3CuO_2 and its structure determination by powder X-ray diffractometry (XRD) method. However, the phase compatibilities in this system have not yet been described.

The oxidation state of copper in the compounds listed above varies from Cu^{+1} to Cu^{+3}. In such a case the method of thermogravimetry (TG) is very informative for establishing the phase diagram. According to the Gibbs' phase rule in thermodynamics [11] ($F = 2 + C - P$ where F the degrees of freedom, C the number of components, and P the number of phases), in a three-component system with one fixed parameter (pO_2) a four-phase equilibrium (3 solids + 1 gas) takes place only for one temperature. Consequently, during heating at a constant rate and fixed pO_2, step-changes of weight should correspond to a three-solid equilibrium (+ 1 gas). Plateaus should correspond to two-solid or single-phase specimens. The required resolution of this method can be achieved by a low heating rate and small amount of sample.

In this paper, we report results obtained by investigations of the Na–Cu–O system using thermogravimetry of $NaCu_2O_2$ and $NaCuO$ compounds as well as X-ray analysis. After a detailed description of the developed synthetic methods, we discuss TG-curves for these two

*Corresponding author. Max-Planck-Institut für Festkörperforschung, Heisenbergstrasse 1, Postfach 800665, Stuttgart D-70569, Germany. Fax: 49-0711-6891093.
*E-mail address:* A.Koulakov@fkf.mpg.de (A.B. Kulakov).

compounds heated in Ar/O_2 gas mixtures with different oxygen partial pressures at 1°C/min. This is followed by an assignment of the plateaus at the TG-curves with the help of X-ray data. We investigate the phase compatibilities in the oxygen-poor part by means of direct synthesis via a specially developed method, followed by X-ray analysis. Finally, we observe the melting and crystallization behavior of $NaCu_2O_2$ and $NaCuO$ under a high temperature microscope.

2. Experimental

Syntheses of $NaCu_2O_2$ were carried out by two methods. In the first method complete reaction of components achieved by addition of about 30 wt% of $Na_2O/NaOH$ eutectic melt with ratio 10/90 mol% as mineralizer analogous to that described by Pickardt et al. [8] for $NaCuO_2$. The starting reagents 6.5 g of Na_2O (97%), 8.6 g of NaOH (99.99%) and 26.5 g of CuO (99.99%) were mixed and transferred into a Pt-crucible (40 mm in diameter) covered with a lid in a dry box. Crucible was heated up to 700°C and annealed at this temperature for 10 h under argon (99.999%) flow and finally cooled down to room temperature. The solidified melt was washed out with dry methanol (0.05% H_2O) to remove the mineralizer. The powder of $NaCu_2O_2$ obtained this way was dried under argon flow.

Also, single-phase samples of $NaCu_2O_2$ and $NaCuO$ were synthesized via the azide/nitrate route (ANR) [12] in specially designed containers [13]. Activated CuO and NaN_3 (Sigma, 99.5%) were used as starting materials. The activated CuO was synthesized by heating $Cu(C_2O_4) \cdot 0.5H_2O$ (Johnson Matthey, 99%) at 350°C in flowing oxygen. The components in ratios according to Eqs. (1) and (2) were ground in a Fritsch planetary ball mill and pressed into pellets ($\varnothing = 13$ mm) under 10^5 N. The pellets were heated first at 150°C for 12 h under vacuum (10^{-6} atm) to remove water and then placed under argon in a tightly closed steel container with a silver inlay

$$2NaN_3 + 4CuO = 2NaCu_2O_2 + 3N_2 \qquad (1)$$

$$2NaN_3 + 2CuO = 2NaCuO + 3N_2. \qquad (2)$$
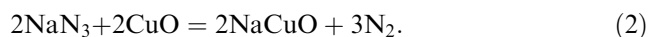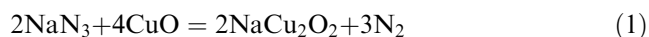
The container was heated up to 260°C, then heated from 260°C to 380°C with heating rate 5°C/h to avoid an explosion of NaN_3 because of exotermick effect during decomposition. The final annealing for the sake of a complete reaction was performed at 500°C for 30 h.

It is well known that Pt-crucibles do not react with Na_2O–NaOH up to 500°C. At higher temperatures, however, a reaction of metallic platinum with the alkaline melt takes place. This process involves the oxidation of Pt and the formation of Pt^{+2} and Pt^{+4} compounds, resulting in platinates of sodium [14].

However, it is possible to use platinum containers for alkaline melts up to 950°C in argon because of the slow kinetics of platinum oxidation.

In order to investigate the processes of oxidation or reduction of compounds thermogravimetrical analyses was performed in a NETZSCH STA-449C system. Small amounts of substances were heated at 1°C/min in a Ar/O_2 gas flow with an oxygen content of 10^{-3}%, 0.2%, 5% and 50%, respectively. The gas flow rate was 10–60 mL/min.

The melting and crystallization behavior of $NaCu_2O_2$ and $NaCuO$ was observed under high-temperature optical microscopy (HTOM) composed of a MS-E1S/VMC-1 (ULVAC-RICO, Japan) infrared image-heating system and a Olympus MS-11 optical microscope. Pt-crucibles $\varnothing$ 3.5×2.2 mm^2 were employed in the experiment. The temperature of the crucible was calibrated by measuring the melting points of Au (1063°C), Ag (960°C), Ge (940°C) and NaCl (800°C).

The powder samples were characterized by X-ray diffractometry using either a STOE Stadi P, or a Philips PW 371 apparatuses with $CuK\alpha_1$ radiation.

The compositions of compounds were examined by the inductively coupled plasma atomic emission spectroscopy (ICP-AES) method using an ARL-3580B analyzer. Preliminary, samples of 5–10 mg weights were dissolved in the *aqua regia*.

3. Results and discussion

3.1. Thermogravimetry and the low-stability limit of the $NaCu_2O_2$ compound

The $NaCu_2O_2$ sample synthesized with the mineralizer is a single-phase, as shown in Fig. 1a. All peaks can be indexed by the JCPDS card 79–2301 of the $NaCu_2O_2$ (Fig. 1b). The deviation of the intensities of the (00L) peaks from the literature data indicates preferential orientation of the powder. The chemical analysis yields a Na/Cu ratio and a small deficiency of oxygen, corresponding to the formula $NaCu_{2.05 \pm 0.05}O_{1.90 \pm 0.05}$.

Fig. 2 shows the TG-curve for $NaCu_2O_2$ during heating in argon (10^{-3}% O_2). Our TG data show that the onset of weight loss starts at about 770°C and continues upto about 1000°C. The rate of decomposition becomes significantly higher at temperatures over 900°C. This rather abrupt increase in the rate of decomposition can be attributed to the appearance of a liquid phase, according to HTOM data (see Table 1). The total weight lost is 4.5 wt%. This value is in good agreement with the one calculated assuming that copper in the liquid phase is completely reduced to Cu^+ (see Eq. (3))

$$NaCu_2O_2 \xrightarrow{T>900°C, 10^{-3}\%O_2} Liquid$$

$$(Na : Cu : O = 1 : 2 : 1.5) + 0.25O_2\uparrow. \qquad (3)$$
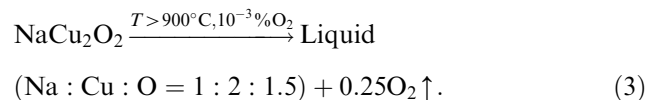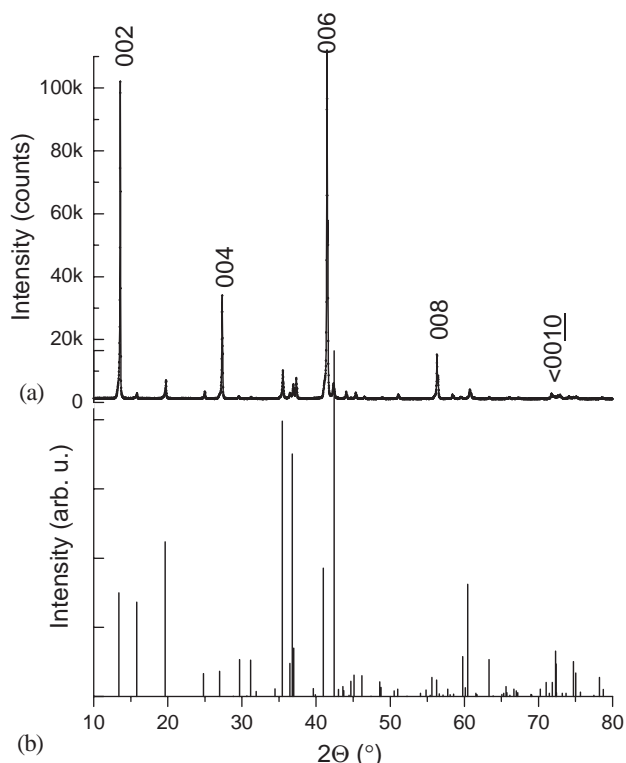
Fig. 1. Powder XRD showing single phase, 00L textured $NaCu_2O_2$ synthesized with mineralizer (a) and JCPDS 79–2301 data (b).
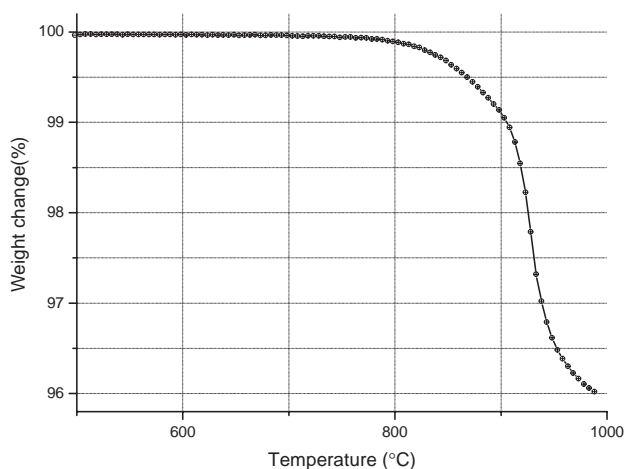

Fig. 2. TG-curve for $NaCu_2O_2$ ($m = 35.51$ mg) heated in argon (10^{-3}% O_2) at 10°C/min.

Table 1
Dependence of incongruent melting points and crystallization temperatures of $NaCu_2O_2$ on oxygen partial pressure determined by HTOM observation

pO_2 (%)	Melting point (°C)	Crystallization (°C)
10^{-3}	905 ± 5	840 ± 5
0.3	905 ± 5	840 ± 5
3	925 ± 5	900 ± 5

The TG-curves of $NaCu_2O_2$ (Fig. 3) demonstrate that the onset of weight increase due to the process of oxidation starts at 150°C. The increase of weight in 0.2% O_2 (curve c) continues up to 530°C. On further heating, weight loss starts and the initial weight (100%) is recovered. This weight recovery is due to the re-synthesis of $NaCu_2O_2$ (according to the X-ray diffraction data of the final product). Evidently, the onset temperature of 530°C is the low-stability limit of $NaCu_2O_2$ in atmosphere with oxygen content 0.2% (Fig. 3).

Analogously, the heating of the $NaCu_2O_2$ in 5% O_2 (curve b) leads to a weight increase followed by plateau in the temperature range of 470–580°C. This is followed by a small step weight loss and another plateau at 620–660°C. Further heating above 660°C again leads to a recovery of the weight to the initial value (100%), corresponding to re-synthesis of $NaCu_2O_2$ (the X-ray diffraction data). These two plateaus at 470–580°C and 620–660°C correspond to the oxidation products of $NaCu_2O_2$ with excess weights of 6.4 and 6.1 wt%, respectively.

Assuming the composition of the initial sample corresponding to the formula $NaCu_2O_2$, we calculate oxygen content as 40 at% (2 atoms of oxygen per 5 atoms in formula unit). Values of oxygen content for the above mentioned two plateaus are 47.6 and 47.3 at% oxygen, correspondingly.

We have prepared another specimen by oxidation of $NaCu_2O_2$ at a constant temperature of 480°C in 5% O_2 for 14 h accompanied by continuous weight measurement in a NETZSCH thermoanalizer as the results are shown in inset of Fig. 3.

Conditions of this isothermal heat treatment correspond to the plateau at 470–580°C at the TG-curve at 1°C/min and the same oxygen content (Fig. 3, curve b). The weight change closed down after 10 h. Fig. 4a shows
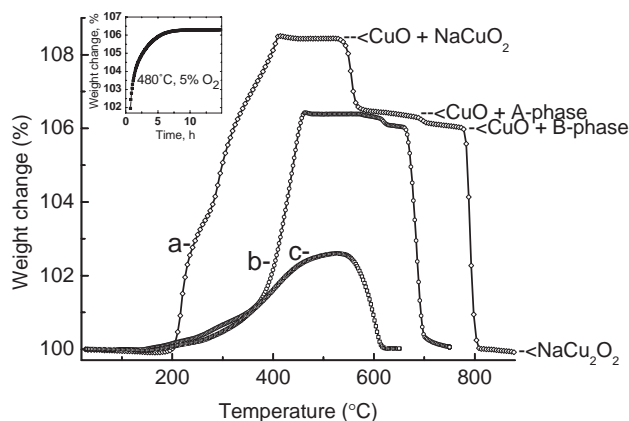

Fig. 3. TG-curves for $NaCu_2O_2$ heated at 1°C/min in gas flow with different oxygen contents: (a) 50% O_2 ($m = 82.434$ mg), (b) 5% O_2 ($m = 71.53$ mg) and (c) 0.2% O_2 ($m = 98.065$ mg). Inset: isothermal TG-curve at 480°C in 5% O_2.
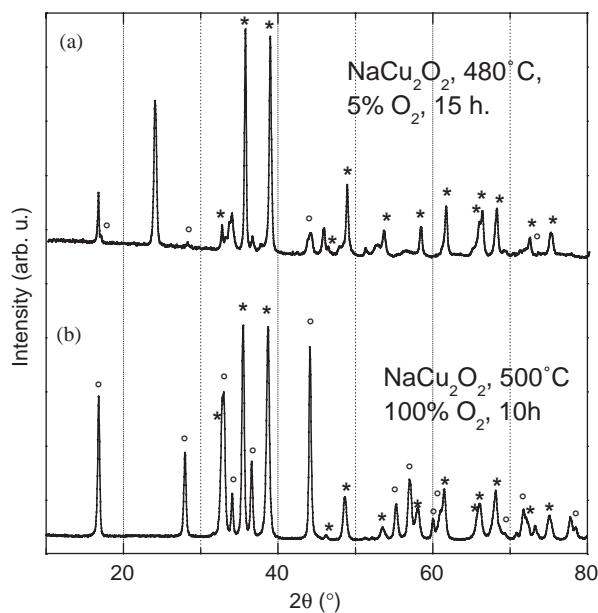
Fig. 4. Powder XRD of products obtained by annealing of $NaCu_2O_2$ under different conditions ($\bigcirc$)—$NaCuO_2$, ($*$)—CuO and unindexed peaks correspond to A-phase.

Fig. 5. Low-stability limit for $NaCu_2O_2$ in pO_2 vs. $1/T$-axes.

the powder diffractogram after this heat treatment, showing a mixture of CuO and an unknown compound (A-phase). The A-phase belongs to the Na-rich part of the phase diagram, because this phase is in equilibrium with CuO and the total cationic ratio Na/Cu = 1/2 remains constant in the sample.

We ascribe the second plateau at 620–660°C to a two-solid equilibrium of CuO + B-phase. The more detailed assignment of the plateaus to the phase equilibria will be given in Section 3.3.

The TG-curve taken upon heating of $NaCu_2O_2$ in 50% O_2 exhibits 4 plateaus (Fig. 3, curve a). Plateaus No. 1–3 will be discussed below together with analogous data for NaCuO in 50% O_2. According to XRD data, the first plateau 400–530°C corresponds to a $NaCuO_2$+CuO mixture (Fig. 4b) and the fourth plateau with onset of 800°C corresponds to re-synthesized $NaCu_2O_2$.

According to the TG-curves of $NaCu_2O_2$ described above (Fig. 3), the onset temperature of weight loss of 530°C in 0.2% O_2, of 660°C in 5% O_2 and of 780°C in 50% O_2 corresponds to re-synthesis of $NaCu_2O_2$ These points lay perfectly on a straight line in a $\lg(pO_2)-1/T$ (K) plot (Fig. 5). Evidently, this line is the low-stability limit of the $NaCu_2O_2$ compound.

3.2. Thermogravimetry of NaCuO compound

The TG-curve of NaCuO in 50% O_2 (Fig. 6, curve a) involves three stages: (1) oxidation with a gain in weight (2) plateau with constant weight and (3) weight loss in 3 steps. Significant oxidation of NaCuO starts at 50°C.
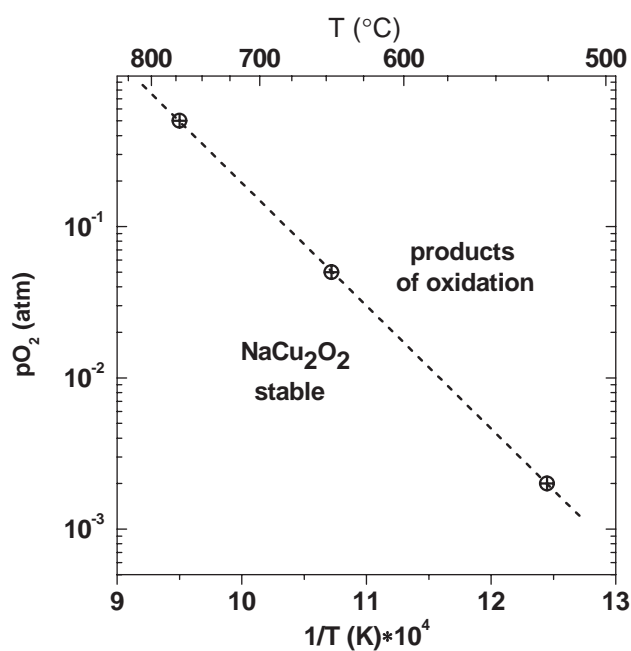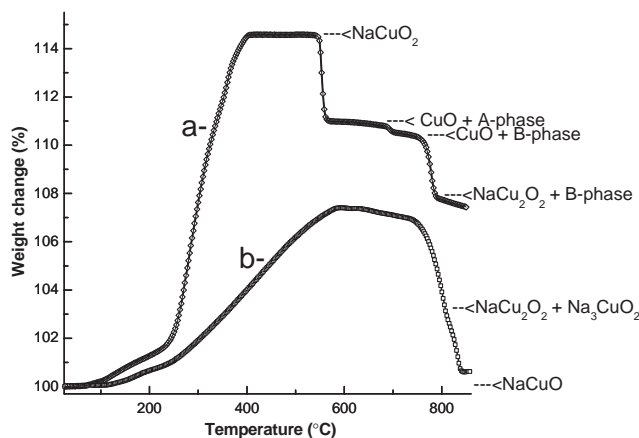

Fig. 6. TG-curves of NaCuO at 1°C/min with different oxygen content: (a) 50% O_2 ($m = 68.92$ mg) and (b) 0.2% O_2 ($m = 92.15$ mg).

The oxidation closes at 400°C, and weight does not change up to 540°C. The calculated value of the weight change for the oxidation of NaCuO to $NaCuO_2$ is 15.6 wt%. The observed weight change is slightly less (14.6 wt%), that is in fair agreement with the calculated one.

In 50% oxygen at temperatures of 540–560°C (Fig. 6, curve a) there is a rather rapid weight loss, indicating that at higher temperatures the $NaCuO_2$ phase is not stable and decomposition takes place. In another words, the point 540°C and 50% O_2 is the upper stability limit of the $NaCuO_2$ phase. At the same oxygen content, re-synthesis of the $NaCu_2O_2$ phase starts with an onset of 780°C, i.e., 240°C higher. Consequently, the onset of

decomposition of the $NaCuO_2$ phase occurs at 240°C before the temperature at which the $NaCu_2O_2$ phase becomes stable. The areas of stability of these two phases do not cross in pO_2-T parameter space. Consequently, the equilibrium of $NaCuO_2$ and $NaCu_2O_2$ phases does not exist, that supports our conclusion about the existence of CuO—A-phase and CuO—B-phase equilibria in this system.

On further heating (Fig. 6, curve a) there are two plateaus: 560–680°C and 700–740°C with a small difference in weight (11.0 and 10.5 wt%, which mean the oxygen content in Na–Cu–O system 46.1 and 45.5 at%, respectively). These two plateaus are similar to the plateaus in the TG-curve for $NaCu_2O_2$ in 50% O_2 and observing around the same temperatures: 570–690°C and 700–780°C (Fig. 3, curve a). For the TG-curve of $NaCu_2O_2$ in 5% O_2, the analogous plateaus are shifted to lower temperatures: 470–580°C and 620–660°C (Fig. 3, curve b). We surmise that these plateaus in the NaCuO and $NaCu_2O_2$ thermograms with small differences in weight correspond to the same two-solid equilibria CuO—A-phase and CuO—B-phase. The correspondence of these plateaus to the mentioned equilibria will also be discussed in the next section.

Further heating leads to rather broad weight loss 740–790°C (Fig. 6, curve a) followed by a slow decrease of weight from +7.9 to +7.4 wt% (43.0–42.5 at% oxygen).

The TG-curve of NaCuO in 0.2% O_2 (Fig. 6, curve b) demonstrates a weight increase up to a maximal value of 7.4 wt% at temperature 590°C. The TG-curve of NaCuO in 50% O_2 reaches nearly the same value of weight at 850°C. Heating from 590°C to 740°C in 0.2% O_2 leads to a slow decrease of weight (from +7.4 to +6.9 wt%). The further weight loss is rather gradual (Fig. 6, curve b) and continues for 100°C (from 740°C to 840°C). For comparison, the weight steps in the TG-curves described above (Figs. 3 and 6 curve a) are much sharper ($\Delta T = 20-30°C$). Such a continuous process indicates that this stage consists of a number (about three) of processes. Regrettably, it is impossible to resolve all stages using a heating rate of 1°C/min. There is a bend at 810°C and a weight value of +3.0 wt% (37.5 at% oxygen), indicating a possible two-solid equilibrium in the narrow temperature interval.

At temperatures higher than 840°C, weight is constant (Fig. 6, curve b) with a small weight excess of 0.6 wt% in comparison with the starting value. XRD of the sample quenched after the TG-measurements exhibits Bragg peaks of NaCuO plus ≈20% of the $NaCu_2O_2$ phase. Such a phase content and the small weight excess mentioned above can be explained by a partial Na-loss as a result of interaction with the Al_2O_3 crucible and formation of $NaCu_2O_2$ (phase with the higher oxygen content).

3.3. Partial Na–Cu–O diagram

As presented in Fig. 7, part of the preliminary Na–Cu–O phase diagram has been established based on the TG-curves described above ("+") and on the XRD data of nine samples synthesized by the ANR ("○"). According to the thermogravimetry data, the decomposition of $NaCu_2O_2$ in an argon atmosphere starts at about 900°C (upper stability limit). Our estimation of the lower stability limit of $NaCu_2O_2$ in 10^{-3}% O_2 gives 380°C. The transition $2CuO = Cu_2O + 1/2O_2$ takes place at this oxygen content at 660°C [1]. As a result, the area of $NaCu_2O_2$ stability in the pO_2-T parameter space intersects with the stability areas of CuO and Cu_2O. This can be easily understood, because the formal oxidation state of copper in $NaCu_2O_2$ (+1.5) is the intermediate between Cu_2O (+1) and CuO (+2). Therefore, the binary equilibria $NaCu_2O_2$–CuO and $NaCu_2O_2$–Cu_2O are established. The CuO–Cu_2O equilibrium is well known [1]. We have thus established a ternary equilibrium $NaCu_2O_2$–CuO–Cu_2O, because no another compound is known inside this triangle.

The equilibrium Cu(met.)—$NaCu_2O_2$ seems to be impossible. As mentioned above, the upper stability limit of the $NaCu_2O_2$ phase in 10^{-3}% O_2 is 900°C. For the transition $Cu_2O = Cu + 1/4O_2$ the temperature 900°C corresponds to 10^{-5}% O_2, i.e., the oxygen content is at least two orders of magnitude lower. The TG data presented above of $NaCu_2O_2$ in 10^{-3}% O_2 and of NaCuO in 0.2% O_2 and direct synthesis via ANR (followed by X-ray characterization) indicate the existence of Cu_2O–NaCuO and $NaCu_2O_2$–NaCuO binary equilibria. Powder XRD of a $NaCu_2O_2$ sample quenched after melting at 900°C in 10^{-3}% O_2 shows peaks of the NaCuO, Cu_2O and $NaCu_2O_2$ phases, which support the existence of binary Cu_2O–NaCuO and $NaCu_2O_2$–Cu_2O–NaCuO ternary equilibria.

Synthesis of the samples via ANR, with compositions corresponding to the two-solid equilibria, demonstrate the existence of the following equilibria: Cu(met.)—NaCuO (Fig. 8b), Cu(met.)—Na_3CuO_2 (Fig. 8b), Cu(met.)—Na_2O (Figs. 8c and e) and NaCuO—Na_3CuO_2 (Fig. 8d) in the oxygen-poor part of the diagram.

XRD of a specimen synthesized by oxidation of $NaCu_2O_2$ in 100% oxygen at 450–500°C demonstrates peaks corresponding to $NaCuO_2$ and CuO phases only (Fig. 4b). This proves the existence of a CuO–$NaCuO_2$ two-solid equilibrium at high oxygen content.

We now discuss the two plateaus with very close values of weights in the thermograms of $NaCu_2O_2$ and NaCuO in 50% O_2 (560–680 and 700–740°C) and 5% O_2 (470–580 and 620–660°C). These plateaus correspond to the following points: Na/Cu = 1/2 (47.6 and 47.3 at% oxygen) and Na/Cu = 1/1 (46.1 and 45.5 at% oxygen) plotted in the Na–Cu–O triangle (denoted as
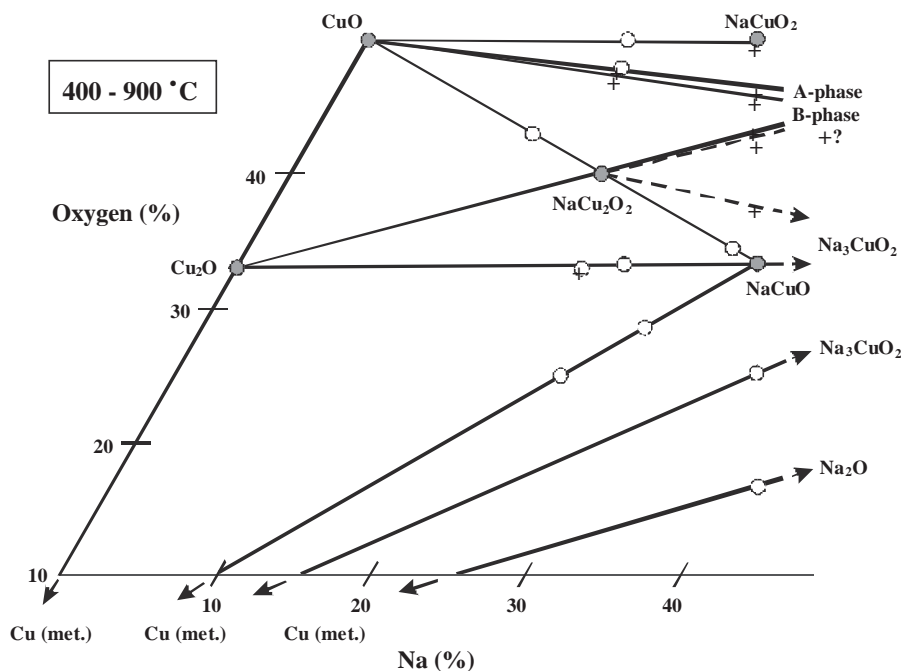
Fig. 7. Preliminary phase diagram for the system Na–Cu–O in the Cu-rich part with experimental data points (($\bullet$) compounds, ($\circ$) synthesis via ANR or quenching after TG with subsequent X-ray, ($+$) plateaus on TG-curves). For conditions of the presented equilibria see the text.
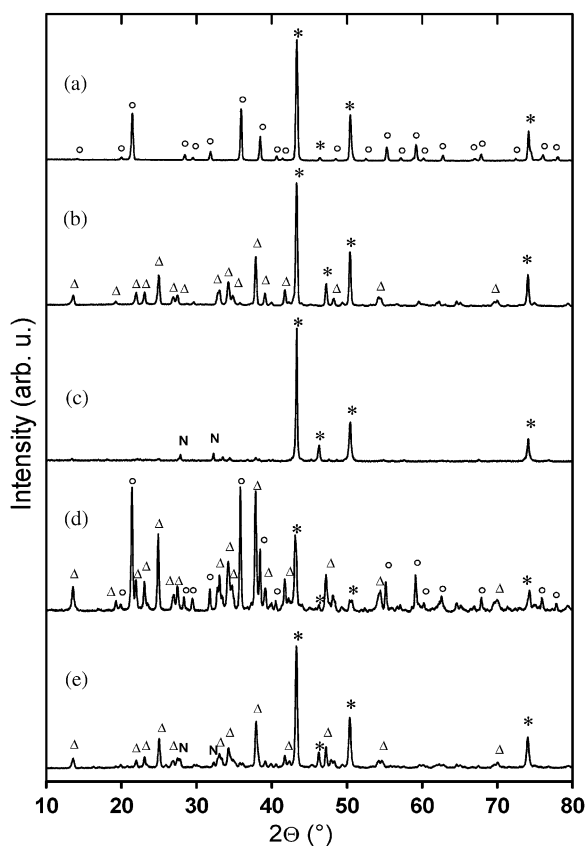

Fig. 8. X-ray diffraction patterns of samples synthesized via ANR with compositions corresponding to the following equilibria: Cu(met.)—NaCuO (a), Cu(met.)—Na$_3$CuO$_2$ (b), Cu(met.)—Na$_2$O (c), Cu(met.)—NaCuO—Na$_3$CuO$_2$ (d) and Cu(met.)—Na$_3$CuO$_2$—Na$_2$O (e) (($*$)—Cu(met.) ($\circ$)—NaCuO, ($\triangle$)—Na$_3$CuO$_2$, N–Na$_2$O).

"$+$" in Fig. 7). These points lie on the two lines starting from the point CuO with good accuracy. These two lines correspond to the CuO—A-phase and CuO—B-phase binary equilibria. As mentioned above, the NaCu$_2$O$_2$ and NaCuO$_2$ phases are not compatible and at least one binary equilibrium (CuO—Na-rich phase) should exist to divide them. We found two such binary equilibria: CuO—A-phase and CuO—B-phase. Consequently the following ternary equilibria should exist: CuO—A-phase-NaCuO$_2$, CuO—A-phase–B-phase and CuO$-$NaCu$_2$O$_2$—B-phase.

We guess, that A- and B-phases are the same to described by Sofin [10] phases with the following formulas Na$_8$Cu$_5$O$_{10}$ and Na$_3$Cu$_2$O$_4$. Single phase specimens of these phases were synthesized and structures of these compounds were solved and refined from X-ray single crystal data by Sofin [10]. So, equilibrium CuO–Na$_6$Cu$_2$O$_6$ does not exists, because the Na$_3$Cu$_2$O$_4$ is positioned exactly at the line between CuO and Na$_6$Cu$_2$O$_6$ phases.

Regrettably, we cannot resolve the part of the diagram between NaCuO$_2$ and NaCuO in the vicinity of the NaCuO phase because the kinetics is very slow and there are a couple of equilibria between the NaCu$_2$O$_2$ phase and unknown phases in the Na-rich part of the diagram. Nevertheless, it is very probable that binary NaCu$_2$O$_2$–Na$_3$CuO$_2$ and ternary NaCu$_2$O$_2$–NaCuO–Na$_3$CuO$_2$ equilibria exist, because on the TG-curve with Na/Cu$=1$ in 0.2% O$_2$ there is hint of a plateau at 810°C corresponding to 37.5 at% oxygen. This point lies on the line connecting the NaCu$_2$O$_2$ and Na$_3$CuO$_2$ phases in the diagram of Fig. 7.

Observations under a high-temperature microscope reveal that the binary eutectic Cu_2O–NaCuO exists with a melting point at about 840°C. The melting point of Cu_2O is 1230°C [1], of Na_2O 1130°C [2], and of NaCuO—according to our observations—higher than 850°C. The $NaCu_2O_2$ phase is stable up to 900°C in 0.3% O_2, that is definitely higher than the Cu_2O–NaCuO eutectic melting point.

For example, at 0.25–0.3% O_2 the NaCuO phase becomes stable according to our TG measurements at temperatures higher than 820°C, the Cu_2O phase according to the equilibrium Cu–O diagram at temperatures higher than 840°C and the $NaCu_2O_2$ phase is stable (TG and high-temperature optical microscopy) in the temperature interval 530–900°C. It may thus be possible to use the melt of the Cu_2O–NaCuO eutectic as flux for the growth of the $NaCu_2O_2$ single crystals [15].

4. Conclusion

Based on our experimental data, the following binary equilibria have been established in the Cu-rich part of the Na–Cu–O diagram: CuO–$NaCuO_2$, CuO–$NaCu_2O_2$, Cu_2O–$NaCu_2O_2$, Cu_2O–NaCuO, $NaCu_2O_2$–NaCuO and Cu(met.)—NaCuO.

A number of binary equilibria have been determined between CuO, $NaCu_2O_2$, NaCuO and Cu(met) phases on the one hand and phases in the Na-rich part of the diagram on the other hand: Cu(met.)—Na_2O, Cu(met.)—Na_3CuO_2, CuO—A-phase, CuO—B-phase, $NaCu_2O_2$–B-phase, $NaCu_2O_2$–Na_3CuO_2 and NaCuO–Na_3CuO_2 and possibly two more binary equilibria, which are impossible to resolve using a the heating rate of 1°C/min. We also found a number of ternary equilibria: CuO–$NaCuO_2$—A-phase, CuO—A-phase–B-phase, CuO–$NaCu_2O_2$—B-phase, Cu_2O−CuO−$NaCu_2O_2$, Cu_2O−$NaCu_2O_2$−NaCuO, Cu(met.)—Cu_2O−NaCuO, Cu(met.)—NaCuO−Na_3CuO_2, Cu(met.)—Na_3CuO_2−Na_2O and $NaCu_2O_2$−NaCuO−Na_3CuO_2.

A high-temperature microscope study and growth experiments show the existence of the binary eutectic Cu_2O–NaCuO with a melting point of about 840°C which can be used as flux for the growth of $NaCu_2O_2$ single crystals.

The low-stability-limit dependence for the $NaCu_2O_2$ phase has been established in a $\lg(pO_2)-1/T$ plot, using the TG-curves upon heating in 0.2%, 5% and 50% O_2.

References

[1] B. Halstedt, D. Risold, L.J. Gauckler, J. Phase Equilibria 15 (1994) 483.
[2] H.A. Wriedt, Bull. Alloy Phase Diagrams 8 (1987) 234.
[3] W. Klein, M. Jansen, Z. Anorg. Allg. Chem. 626 (2000) 136.
[4] R. Hoppe, K. Hestermann, F. Schenk, Z. Anorg. Allg. Chem. 367 (1969) 275.
[5] G. Tams, Hk. Müller-Buschbaum, J. Alloys Compds. 189 (1992) 241.
[6] K. Hestermann, R. Hoppe, Z. Anorg. Allg. Chem. 367 (1969) 261.
[7] N.E. Brese, M. O'Keeffe, R.B. von Dreele, V.G. Young Jr., J. Solid State Chem. 83 (1989) 1.
[8] J. Pickardt, W. Paulus, M. Schmalz, L. Schöllhorn, J. Solid State Chem. 89 (1990) 308.
[9] N. Bukovec, I. Leban, R. Hoppe, Z. Anorg. Allg. Chem. 563 (1988) 79.
[10] M. Sofin, Ph.D. Dissertation, Max-Planck-Institute für Festkörperforschung, Stuttgart, 2003.
[11] C.H.P. Lupis, Chemical Thermodynamics of Materials. Elsevier Sci. Publ., Amsterdam, 1983, p. 68.
[12] D. Trinschek, M. Jansen, Angew. Chem. 111 (1999) 234; D. Trinschek, M. Jansen, Angew. Chem. Int. Ed. Engl. 38 (1999) 133.
[13] M. Sofin, E.M. Peters, M. Jansen, Z. Anorg. Allg. Chem. 628 (2002) 2697.
[14] W. Urland, R. Hoppe, Z. Anorg. Allg. Chem. 392 (1972) 23.
[15] A. Maljuk, A.B. Kulakov, M. Sofin, L. Capogna, J. Stempfer, C.T. Lin, M. Jansen, B. Keimer, J. Cryst. Growth 263 (2004) 338.